



Necroptosis Underlies Hepatic Damage in a Piglet Model of Lipopolysaccharide-Induced Sepsis

OPEN ACCESS

Edited by:

Saurabh Chatterjee,
University of South Carolina,
United States

Reviewed by:

Shuo Xiao,
Rutgers, The State University of New
Jersey - Busch Campus,
United States
Ayan Mondal,
University of South Carolina,
United States

*Correspondence:

Yulan Liu
yulanflower@126.com

†These authors have contributed
equally to this work

Specialty section:

This article was submitted to
Inflammation,
a section of the journal
Frontiers in Immunology

Received: 27 November 2020

Accepted: 25 February 2021

Published: 12 March 2021

Citation:

Xu Q, Guo J, Li X,
Wang Y, Wang D, Xiao K,
Zhu H, Wang X, Hu C-AA,
Zhang G and Liu Y (2021)
Necroptosis Underlies Hepatic
Damage in a Piglet Model of
Lipopolysaccharide
-Induced Sepsis.
Front. Immunol. 12:633830.
doi: 10.3389/fimmu.2021.633830

Qiao Xu^{1†}, Junjie Guo^{1†}, Xiangen Li¹, Yang Wang¹, Dan Wang¹, Kan Xiao¹, Huiling Zhu¹,
Xiuying Wang¹, Chien-An Andy Hu^{1,2}, Guolong Zhang^{1,3} and Yulan Liu^{1*}

¹ Hubei Key Laboratory of Animal Nutrition and Feed Science, Wuhan Polytechnic University, Wuhan, China, ² Department of Biochemistry and Molecular Biology, University of New Mexico School of Medicine, Albuquerque, NM, United States,

³ Department of Animal and Food Sciences, Oklahoma State University, Stillwater, OK, United States

Background: Necroptosis is a newly recognized form of programmed cell death with characteristics of both necrosis and apoptosis. The role of necroptosis in hepatic damage during sepsis is poorly understood. In this study, we investigated the occurrence of necroptosis in hepatic damage, and its contribution to hepatic damage in a piglet model of lipopolysaccharide (LPS)-induced sepsis.

Methods: Two animal experiments were conducted. In trial 1, piglets were challenged with LPS and sacrificed at different time points after LPS challenge. In trial 2, piglets were pretreated with necrostatin-1, a specific inhibitor of necroptosis, prior to LPS challenge. Alterations in the hepatic structure and function, pro-inflammatory cytokine expression, and the necroptosis signaling pathway were investigated. Typical ultrastructural characteristics of cell necrosis was observed in the liver of LPS-challenged piglets.

Results: Expressions of critical components of necroptosis including kinases (RIP1, RIP3, and MLKL), mitochondrial proteins (PGAM5 and DRP1), and an intracellular damage-associated molecular pattern (HMGB1) were increased in the liver in a time-dependent manner, followed by hepatic inflammation, morphological damage, and dysfunction as manifested by elevated hepatic expression of IL-1 β , IL-6 and TNF- α as well as increased serum AST and AKP activities and the AST/ALT ratio. Pretreatment with necrostatin-1 significantly reduced the expression of RIP1, RIP3 and MLKL as well as PGAM5, DRP1 and HMGB1, which subsequently led to obvious attenuation of hepatic inflammation and damage.

Conclusions: Our study demonstrates that necroptosis occurs in the liver during sepsis and contributes to septic hepatic injury.

Keywords: necroptosis, liver injury, sepsis, necrostatin-1, pigs, lipopolysaccharide

INTRODUCTION

Sepsis is a common and life-threatening illness that could lead to multiple organ failure, shock, and death as a result of an exaggerated inflammatory response to infection (1, 2). As a main cause of deaths in intensive care units, sepsis accounts for an estimated 200,000 deaths annually in the US alone (3). The liver is a target tissue frequently damaged by sepsis (4). Severe septic liver damage may further cause multiple organ dysfunction syndrome (5). It is important to understand the mechanism of septic hepatic injury before devising effective therapeutic strategies.

Hepatic cell death is a critical event in progression of various liver diseases (6, 7). Traditionally, apoptosis and necrosis are recognized as two main modes of cell death contributing to the pathogenesis of liver diseases (7). In recent years, necroptosis, a novel mode of cell death, has been identified (8, 9). Necroptosis incorporates features of both necrosis and apoptosis, and is strictly regulated by receptor interacting protein kinase (RIP) 1 and 3 (9, 10). Auto- and transphosphorylations of RIP1 and RIP3 are required for assembly of RIP1/3-containing necrosome and activation of necroptotic signaling (9, 11). RIP3 subsequently recruits and phosphorylates mixed lineage kinase domain-like protein (MLKL) to promote its oligomerization and translocation to plasma membrane, resulting in membrane rupture and necrotic cell death (9). In addition, the RIP1/3-containing necrosome has also been reported to activate the mitochondrial phosphatase phosphoglycerate mutase family member 5 (PGAM5), which recruits and activates the mitochondrial fission factor dynamin-related protein 1 (DRP1) (12, 13). Activation of DRP1 results in mitochondrial fragmentation and reactive oxygen species generation, resulting in necrotic cell death (14). Cell rupture and necrosis lead to the release of intracellular damage-associated molecular patterns (DAMP) such as high-mobility group box 1 (HMGB1) protein, which triggers inflammation and secondary tissue damage (15).

Accumulating evidence has indicated that necroptosis plays a crucial role in several forms of liver injury in mice such as alcoholic liver disease (16), non-alcoholic fatty liver disease (17) and liver ischemia-reperfusion injury (18). However, the role of necroptosis in septic liver injury is rarely investigated. Pig is an excellent model for human physiology and pathology (19, 20). In the present study, we employed a piglet model of LPS-mediated sepsis (21, 22), to confirm the occurrence of necroptosis in the liver. The contribution of necroptosis to liver damage was further explored by pretreatment of animals with necrostatin-1 (Nec-1), a well-described inhibitor of necroptosis (23), prior to LPS challenge.

Abbreviations: AKP, alkaline phosphatase; ALT, alanine aminotransferase; AST, aspartate aminotransferase; BW, body weight; DAMP, damage-associated molecular pattern; IL, interleukin; DRP1, dynamin-related protein 1; LPS, lipopolysaccharide; MLKL, mixed-lineage kinase domain-like protein; Nec-1, necrostatin-1; PAMP, pathogen associated molecular pattern; PGAM5, phosphoglycerate mutase family member 5; RIP, receptor interacting protein kinase; TNF- α , tumor necrosis factor- α ; HMGB1, high-mobility group box 1.

METHODS

Animals and Experimental Design

Animal experimental procedures were approved by the Animal Care and Use Committee of Wuhan Polytechnic University (Wuhan, China). A total of 70 weaned, apparently healthy piglets (Duroc \times Large White \times Landrace, 28 ± 3 d, average body weight of 7.1 ± 0.9 kg) were purchased from Aodeng Agricultural and Animal Husbandry Technology Co., Ltd (Hubei, China). The pigs were individually housed in 1.80×1.10 m² pens, maintained in an environmentally controlled room, and received a standard weanling piglet diet for acclimation for 14 d with free access to feed and water. Animals were observed daily for signs of diarrhea, sickness, and abnormal behavior.

In the first experiment, 42 weanling piglets were randomly allocated to seven groups including a control group and six LPS groups slaughtered at six different time points. Each group had six piglets. The piglets in LPS groups were injected intraperitoneally with *Escherichia coli* LPS (*Escherichia coli* serotype 055: B5, MilliporeSigma, St. Louis, MO, USA) at 100 μ g/kg body weight (BW) and then were slaughtered at 1, 2, 4, 8, 12, or 24 h after LPS challenge (**Table 1S**). The piglets in the control group were slaughtered right (0 h) after injection with an equivalent volume of sterile saline. The dose of LPS administered was shown to trigger an obvious inflammatory response and sepsis based on our earlier experiments (22, 24).

In the second experiment, 28 weanling piglets were randomly assigned to four groups in a 2×2 factorial design with seven piglets in each group. The animals were pretreated intraperitoneally with Nec-1 (MedChem Express, NJ, USA) at 1.0 mg/kg BW or an equivalent volume of 2% DMSO 30 min before intraperitoneal injection of LPS at 100 μ g/kg BW or saline (**Table 2S**). The piglets were killed at 4 h after LPS or saline injection.

Blood and Liver Sample Collection

Prior to animal sacrifice, blood samples were collected into 10-mL vacuum tubes (Becton Dickinson Vacutainer Systems; Franklin Lakes, NJ, USA) *via* jugular vein puncture, and centrifuged at 3,500 g for 10 min to collect serum. Serum was stored at -80°C until analysis. Following blood collection, the pigs were humanely euthanized with an intramuscular injection of sodium pentobarbital (80 mg/kg BW), and then the liver samples (0.5 cm³ segments) were harvested. One portion of the liver samples was fixed in fresh 4% paraformaldehyde/phosphate-buffered saline for 24 h for histological analysis. Another portion was cut into smaller pieces (about 1 mm³) and fixed with 2.5% glutaraldehyde at 4°C for ultrastructural transmission electron microscopy (TEM) analysis. The remaining liver tissue was diced into smaller pieces, snap frozen in liquid nitrogen, and stored at -80°C for further analysis.

Biochemical Measurements of the Serum Samples

The activities of alanine aminotransferase (ALT), aspartate aminotransferase (AST) and alkaline phosphatase (AKP) in the

serum were determined using a colorimetric method with commercial kits (Nanjing Jiancheng Biological Product, Nanjing, China) according to the manufacturer's instructions.

Liver Histological Analysis

After a 24-h fixation, liver segments (5-mm) were dehydrated with a series of increasing concentrations of ethanol, cleared with xylene, and embedded in paraffin. Cross-sections (4- μ m thick) of each sample were deparaffinized, and stained with hematoxylin and eosin. Histological analysis was performed in a blinded manner by an experienced pathologist using a light microscope with a computer-assisted morphometric system (BioScan Optimetric, BioScan, Edmonds, WA, USA).

Liver Ultrastructural Analysis

Liver samples were fixed with 2.5% glutaraldehyde, and postfixed in 1% osmium tetroxide. They were then dehydrated with ethanol and embedded in Epon 812 (Eimicon, Shanghai, China). Ultra-thin sections (100 nm) were cut and stained with uranyl acetate and lead citrate. Ultrastructural observation was conducted in a blinded manner by an experienced pathologist using a transmission electron microscope (TEM) (Tecnai, FEL, Hillsboro, USA) at an accelerating voltage of 200 kV and a magnification of 5,000.

Measurement of Proinflammatory Cytokine Concentrations

Frozen liver samples were weighed, homogenized in nine volumes of ice-cold saline solution, and centrifuged at 2,500 rpm for 10 min at 4°C to collect the supernatants. The protein concentrations of the supernatants were measured using the bicinchoninic acid reagent (Applygen Technologies Co., China). The concentrations of tumor necrosis factor- α (TNF- α), interleukin (IL)-6 and IL-1 β in the supernatants were determined using respective ELISA kits (R&D Systems, Minneapolis, MN, USA) according to the manufacturer's protocols and expressed as pg/mg protein.

Protein Expression Analysis by Western Blot

Liver samples (100-150 mg) were suspended in lysis buffer, homogenized, and centrifuged to collect the supernatants. Protein concentrations of the supernatants were measured using the bicinchoninic acid reagent (Applygen Technologies Co., China). Equal amounts of hepatic proteins were loaded and separated on a polyacrylamide gel and transferred onto polyvinylidene difluoride membranes. Immunoblots were blocked for at least 1 h with 3% bovine serum albumin in TBS/Tween-20 buffer. The membranes were incubated overnight at 4°C with primary antibodies and then with the horseradish peroxidase-labelled secondary antibodies for 2 h at room temperature. Specific primary antibodies included rabbit anti-RIP1 (#LS-B8214, LifeSpan), rabbit anti-RIP3 (#SC-135170, Santa Cruz), rabbit anti-phosphorylated MLKL (p-MLKL) (#62233, Cell Signaling), rabbit anti-PGAM5 (#ab131552, Abcam), rabbit anti-DRP1 (#ab154879, Abcam), rabbit

anti-HMGB1 (#PAB12414, Abnova), and mouse anti- β -actin (#A2228, Sigma Aldrich). Blots were developed using an Enhanced Chemiluminescence Western blotting kit (Amersham Biosciences, Sweden), visualized using a Gene Genome Bioimaging System, and analyzed using GeneTools software (Syngene, Frederick, MD, USA). The relative protein abundance of target proteins were expressed as the ratio of target protein/ β -actin protein.

mRNA Expression Analysis by Real-Time PCR

Total RNA was isolated from the liver samples by using TRIzol (TaKaRa Biotechnology Co., Dalian, China) and quantified using Nano-Drop 2000 Spectrophotometer (Thermo Scientific, Wilmington, DE, USA). RNA purity was assessed by determining the ratio of the absorbance at 260 and 280 nm, and the integrity was verified using agarose gel electrophoresis. Genomic DNA removal and cDNA synthesis were performed using PrimeScript[®] RT Kit (TaKaRa Biotechnology). Real-time PCR analysis was performed using a SYBR[®] Premix Ex Taq[™] (Tli RNaseH Plus) qPCR kit (TaKaRa Biotechnology) on an Applied Biosystems 7500 Real-Time PCR System (Applied Biosystems, Life Technologies). The total volume of each PCR reaction was 20 μ L, which contained 10.0 μ L SYBR[®] Premix Ex Taq[™], 0.4 μ L forward primer (10 μ mol/L), 0.4 μ L reverse primer (10 μ mol/L), 0.4 μ L ROX reference dye II (10 \times), 2.0 μ L cDNA and 6.8 μ L RNase-free water. After an initial denaturation at 95°C for 30 s, the reaction was cycled at 95°C for 5 s and 60°C for 34 s for 40 times. The primer pairs used are shown in **Table 1**. The expression level of each target gene relative to a reference gene (GAPDH) was analyzed using the $2^{-\Delta\Delta Ct}$ method of Livak and Schmittgen (25). Our results demonstrated that GAPDH did not exhibit any variation among treatments. Relative mRNA abundance of each target gene was expressed as the fold change of its expression level in an experimental sample over that in control samples.

Statistical Analysis

In the first experiment, the data were analyzed using Duncan's multiple comparison tests. In the second experiment, the data were analyzed using the general linear model procedures of

TABLE 1 | Primer sequences used in real-time PCR.

Gene	Forward (5'-3')	Reverse (5'-3')
TNF- α	AAGACACCATGAGCACTGAGA	CGACCAGGAGGAAGGAGAAG
IL-1 β	GCTAACTACGGTGACAACAATAATG	CTTCTCCACTGCCACGATGA
IL-6	AAGGTGATGCCACCTCAGAC	TCTGCCAGTACCTCCTTGCT
RIP1	ACATCCTGTACGGCAACTCT	CGGGTCCAGGTGTTTATCC
RIP3	CTTGTTGTCTGTCCGTGAGC	GAGGAGGTTGGGCTGTTGA
MLKL	TCTCGCTGCTGCTTCA	CTCGCTTGCTTCTCTCTG
PGAM5	TCTTCATCTGCCACGCCAAT	GGTGATGCTGCCGTTGTTG
DRP1	TGTGGCTGCAGGTCATTA	TTGCCCTGGGACATTTTATGC
HMGB1	GCCTATCCATTGGTGATGTTG	TCCTCCTCCTCCTCCTCAT
GAPDH	CGTCCCTGAGACACGATGGT	GCCTTGACTGTGCCGTGGAAT

DRP1, dynamin-related protein 1; *HMGB1*, high-mobility group box 1; *IL*, interleukin; *MLKL*, mixed-lineage kinase domain-like protein; *PGAM5*, phosphoglycerate mutase family member 5; *RIP*, receptor interacting protein kinase; *TNF- α* , tumor necrosis factor- α .

ANOVA (SAS, Cary, NC, USA). Post hoc testing was conducted using Duncan's multiple comparison tests. All data were presented as means ± standard errors of the mean. $P \leq 0.05$ was considered statistically significant.

RESULTS

Hepatic Damage and Dysfunction Are Dynamically Induced in LPS-Challenged Piglets

To investigate the dynamic effect of LPS on the liver, we examined hepatic histopathological changes of pigs at 1, 2, 4,

8, 12, and 24 h after LPS challenge. Compared to the control pigs (0 h), LPS-challenged pigs displayed a progressive increase in liver damage as manifested by disordered hepatic cell cord arrangement, inflammatory cell infiltration, and karyolysis, karyopyknosis, and vacuolation of hepatocytes (**Figure 1A**). Hepatic injury gradually increased between 1-4 h, became severe between 4-12 h and alleviated obviously at 24 h.

To explore the dynamic effect of LPS challenge on hepatic function, we measured the activities of AST, ALT and AKP in the serum (**Figures 1B-E**), which are commonly used makers of hepatic function (22, 24). LPS challenge increased serum AST activity between 4-24 h (peaking at 8 h), the AST/ALT ratio between 4-24 h (peaking at 8 h), and the AKP activity between

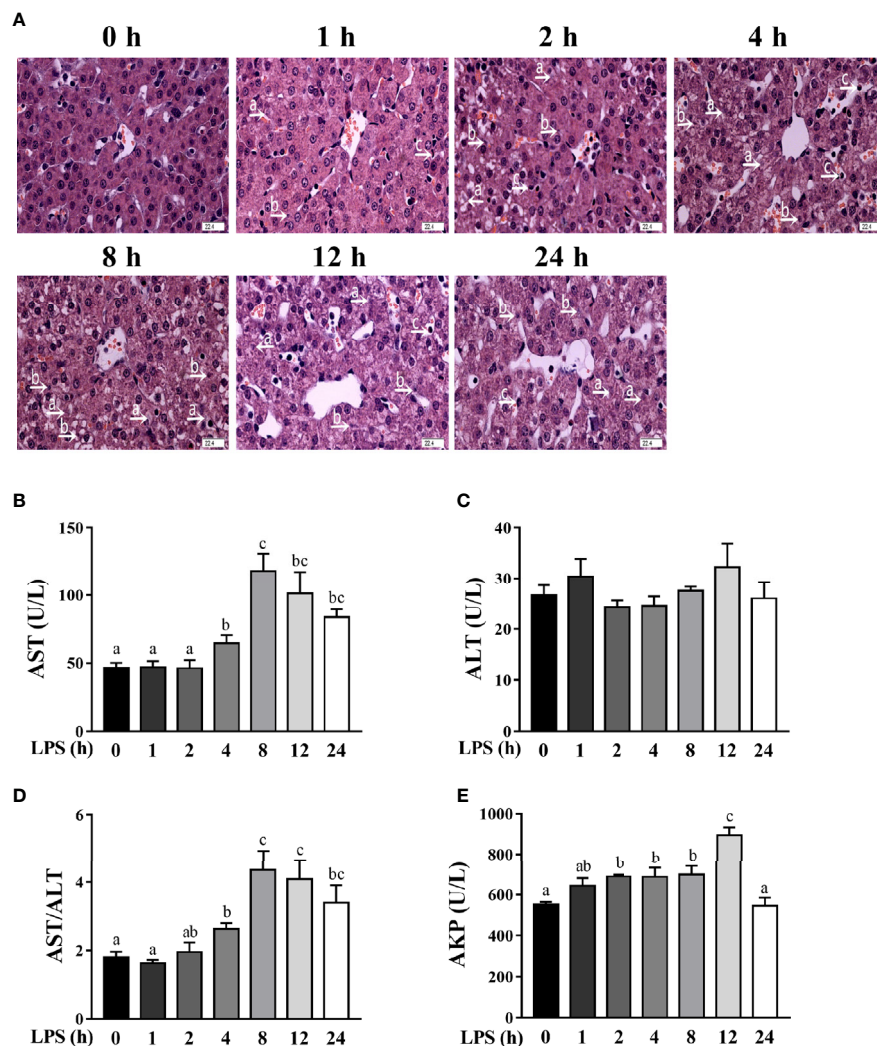


FIGURE 1 | Hepatic damage and dysfunction are dynamically induced in LPS-challenged piglets. Piglets were sacrificed right after injection with sterile saline and served as controls (0 h), while others were challenged with LPS at 100 µg/kg body weight and sacrificed at 1, 2, 4, 8, 12, or 24 h after challenge. **(A)** Representative haematoxylin/eosin-stained liver sections of the control (Con) group and LPS groups. Karyolysis (a) and karyopyknosis (b) of hepatocytes, inflammatory cell infiltration (c), disordered hepatic cell cord arrangement, and hepatocyte vacuolation were observed in LPS-challenged samples. Magnification: 400 ×, scale bars = 22.4 µm. **(B-E)** Serum AST, ALT and AKP activities and the AST/ALT ratio. Values are means ± SEM, n = 6. ^{abc} Means without a common letter differ significantly ($p < 0.05$).

2-12 h (peaking at 12 h) ($p < 0.05$). However, LPS had no effect on serum ALT activity.

Hepatic Inflammation Is Dynamically Induced in LPS-Challenged Piglets

Hepatic inflammation contributes to hepatic damage (22, 24). To investigate the dynamic effect of LPS on hepatic inflammatory response of pigs, we analyzed mRNA and protein levels of hepatic pro-inflammatory cytokines including TNF- α , IL-6 and IL-1 β (Figures 2A, B). LPS challenge triggered a marked, but temporary increase of these pro-inflammatory cytokines. Specifically, mRNA expression levels of TNF- α , IL-6, and IL-1 β were elevated between 1-12 h, peaked at 1 h, and returned to the basal levels at 24 h. Similarly, LPS elevated protein concentrations of TNF- α between 1-2 h (peaking at 1 h), IL-6 at 2 h, and IL-1 β between 1-24 h (peaking at 4 h) ($p < 0.05$).

Hepatic Cell Necroptosis Is Dynamically Induced in LPS-Challenged Piglets

To explore if necroptosis occurred concomitant with hepatic injury and inflammation in LPS-challenged pigs, we examined liver ultrastructure by TEM (Figure 3A). Compared to the control pigs, LPS-challenged pigs exhibited significant hepatic

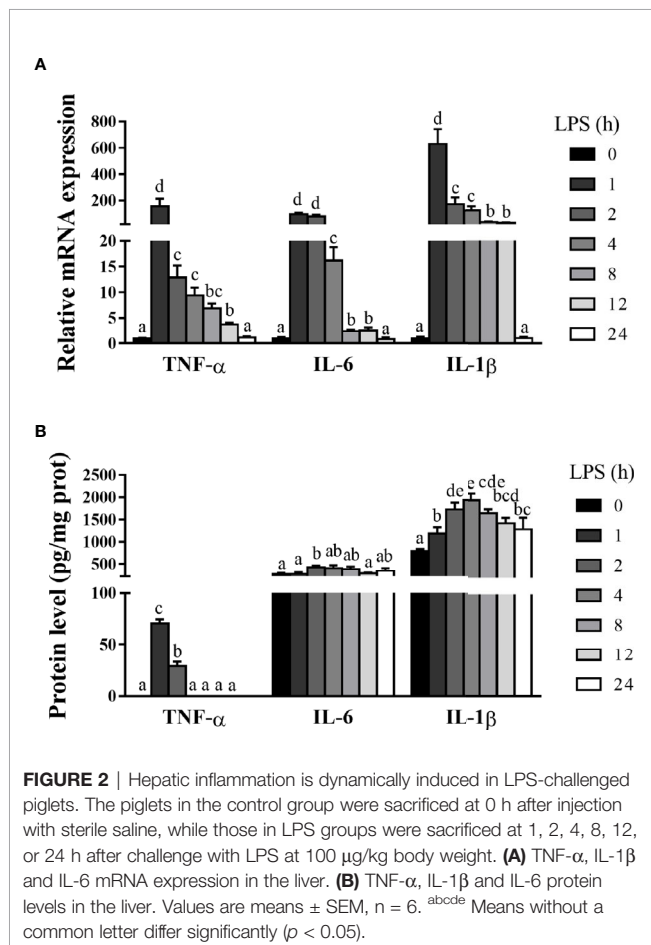
ultrastructure damages showing mitochondrial swelling, endoplasmic reticulum expansion, nuclear deformation, nuclear membrane rupture, and chromatin overflow. To further explore the occurrence of necroptosis in septic liver, we measured the mRNA and protein levels of important components of necroptosis including RIP1, RIP3 and MLKL, PGAM5, DRP1, and HMGB1 (Figures 3B-I). As compared to the control group, LPS triggered a time-dependent up-regulation of RIP1, RIP3, MLKL, PGAM5, and DRP1 in the liver. Specifically, LPS increased the mRNA level of RIP1 between 2-12 h (peaking at 4 h and 5.12 fold), RIP3 between 8-12 h (peaking at 8 h and 2.04 fold), MLKL between 2-4 h (peaking at 4 h and 6.39 fold), PGAM5 between 4-8 h (peaking at 4 h and 4.72 fold) and DRP1 at 4 h (3.71 fold) ($p < 0.05$). However, LPS decreased mRNA abundance of HMGB1 at 1, 2, 4 and 24 h. Similarly, LPS elevated protein abundance of RIP1, RIP3 and phosphorylated MLKL between 2-24 h, and PGAM5 between 8-24 h and DRP1 between 4-24 h, peaking at 8, 4, 12, 12, 8 or 4 h, respectively ($p < 0.05$). Inconsistent with mRNA expression, protein abundance of HMGB1 was increased at 2, 4, 12 and 24 h ($p < 0.05$). These results, in combination with the severity of hepatic injury and inflammation, indicated that 4 h post LPS challenge is the time when the liver is experiencing dramatic changes and therefore, was chosen for analysis of the hepatic function and damage in a subsequent animal trial.

Nec-1 Inhibits Hepatic Necroptosis in LPS-Challenged Piglets

To further demonstrate that LPS-induced hepatic damage is partially due to necroptosis, the piglets were pretreated with Nec-1, which is a specific inhibitor of RIP1 kinase activity (23) and RIP1/RIP3 association (11), 30 min prior to LPS challenge. TEM of the liver revealed that Nec-1 reduced LPS-triggered necrotic ultrastructural alterations (Figure 4A). LPS challenge for 4 h increased mRNA expression levels of RIP1, MLKL, PGAM5, and DRP1 and protein expression of RIP1, RIP3, phosphorylated MLKL, PGAM5, DRP1, and HMGB1 ($p < 0.05$) (Figures 4B-I). However, Nec-1 pretreatment reversed LPS-induced mRNA expression of RIP1, MLKL, PGAM5, and DRP1 as well as protein expression of RIP1, RIP3, phosphorylated MLKL, PGAM5, DRP1, and HMGB1 ($p < 0.05$).

Nec-1 Alleviates Hepatic Damage, Dysfunction, and Inflammation in LPS-Challenged Piglets

We examined whether Nec-1 pretreatment could alleviate LPS-induced hepatic damage and dysfunction. Indeed, inhibition of necroptosis by Nec-1 obviously attenuated morphological damage in the liver 4 h post LPS challenge (Figure 5A). Desirably, Nec-1 largely restored the activities of AST, ALT, and AKP as well as the AST/ALT ratio in the serum of LPS-challenged piglets to basal levels (Figures 5B-E). Consistently, inhibition of necroptosis by Nec-1 significantly attenuated LPS-mediated induction of the mRNA expression levels of TNF- α and IL-6, but not IL-1 β , in the liver ($p < 0.05$) (Figures 6A-C).



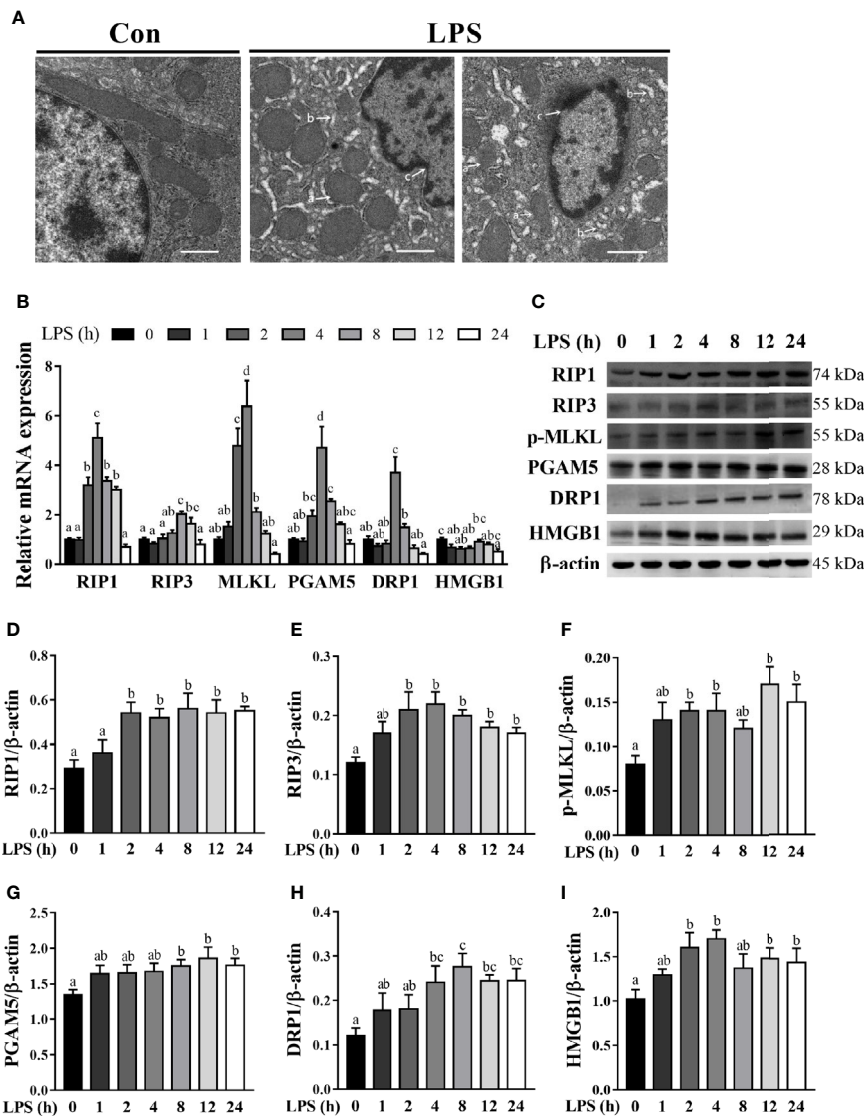


FIGURE 3 | Hepatic cell necroptosis is dynamically induced in LPS-challenged piglets. The piglets in the control (Con) group were sacrificed at 0 h after injection with sterile saline, while those in LPS groups were sacrificed at 1, 2, 4, 8, 12, or 24 h after challenge with LPS at 100 μg/kg body weight. **(A)** Representative hepatic ultrastructures in Con and LPS groups. The liver sections were imaged using transmission electron microscopy. It is noted that mitochondrial swelling (a) and endoplasmic reticulum expansion (b) as well as nuclear deformation, nuclear membrane rupture, and chromatin overflow (c) were observed in LPS groups. Magnification: 5000 ×, scale bars = 1 μm. **(B)** mRNA abundance of necroptosis signaling components in the liver. **(C–I)** Protein abundance of necroptosis signaling components in the liver. Values are means ± SEM, n = 6. ^{abcd} Means without a common letter differ significantly (p < 0.05).

DISCUSSION

In addition to necrosis and apoptosis, a novel mode of cell death namely necroptosis was recently identified (8, 9). Necroptosis has similar morphological characteristics with necrosis, but is strictly controlled by an intracellular protein platform, similar to apoptosis (9, 10). Emerging evidence has indicated that necroptosis is implicated in the pathogenesis of alcoholic liver disease (16), non-alcoholic fatty liver disease (17), and ischemia-reperfusion injury of steatotic livers (18, 26). However, the

involvement of necroptosis in septic liver injury is largely unknown.

In the current study, we evaluated the dynamic effect of LPS on hepatic damage in a piglet model. Hepatic injury has been found to be gradually increased up to 12 h post LPS challenge, and obviously diminished at 24 h. It is not surprising to observe concomitant hepatic dysfunction associated with hepatic histopathological changes. Serum AST and AKP activities as well as the AST/ALT ratio were evidently increased between 4–24 h post LPS challenge. These results are in agreement with our

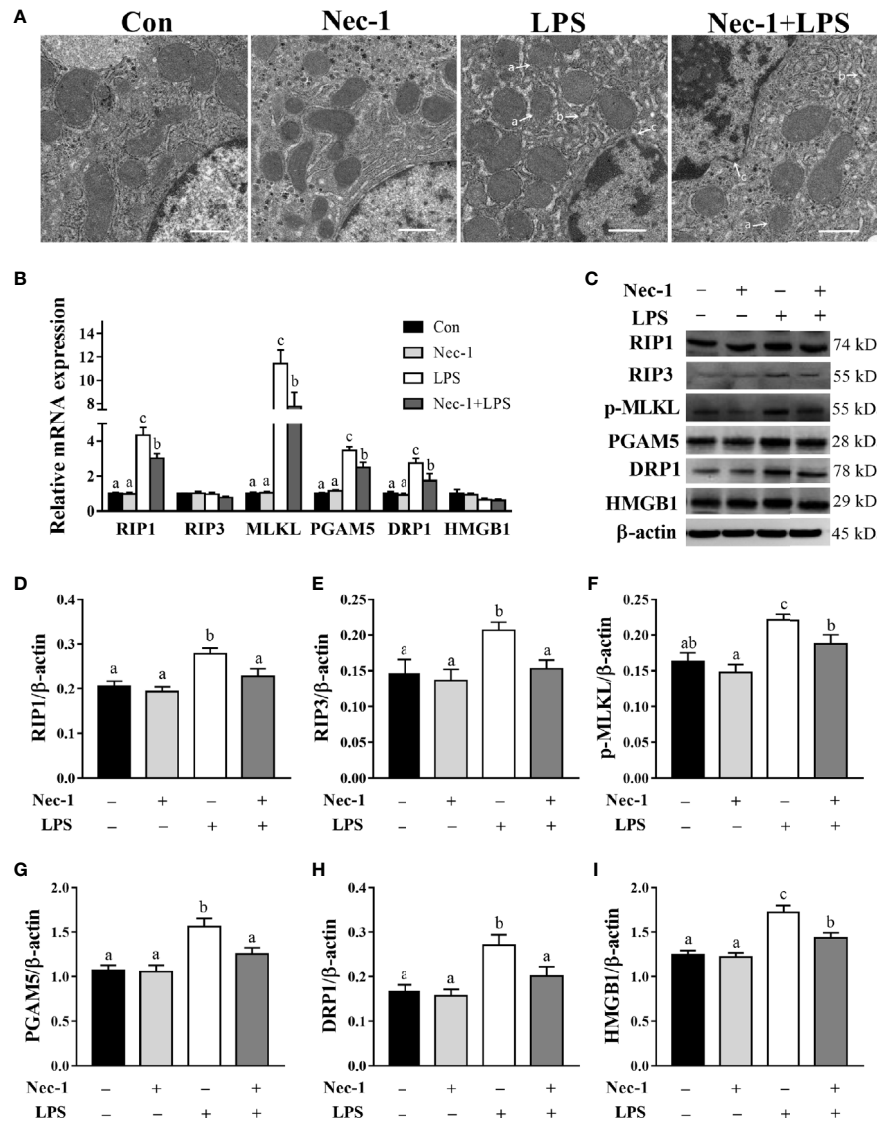


FIGURE 4 | Necrostatin-1 (Nec-1) inhibits hepatic necroptosis in LPS-challenged piglets. Piglets were pretreated with Nec-1 at 1.0 mg/kg body weight or an equal volume of 2% DMSO 30 min before LPS or saline administration. Pigs were sacrificed at 4 h after LPS or saline injection. **(A)** Representative hepatic ultrastructural images by transmission electron microscopy. LPS caused significant necrosis such as mitochondrial swelling (a), endoplasmic reticulum expansion (b), nuclear deformation, nuclear membrane rupture and chromatin overflow (c), while Nec-1 markedly reduced the necrotic ultrastructural changes. Magnification: 5000 ×, scale bars = 1 μm. **(B)** mRNA abundance of necroptosis signaling components in the liver. **(C–I)** Protein abundance of necroptosis signaling components in the liver. Values are means ± SEM, n = 7. ^{abc} Means without a common letter differ significantly (p < 0.05).

previous reports on a piglet model of LPS-induced sepsis; however, those studies only studied a single time point (4 or 24 h) after LPS challenge (22, 24).

Hepatic injury is closely associated with hepatic inflammation (22, 24). As expected, LPS evoked a marked increase of several representative pro-inflammatory cytokines such as TNF-α, IL-6 and IL-1β at both mRNA and protein levels. TNF-α, IL-6, and IL-1β mRNA expression levels in the liver were quickly peaked at 1 h after LPS challenge, while their protein levels were peaked within 4 h. The temporal patterns of LPS-induced changes of

these cytokines are consistent with a previous observation in rats (27).

Given the fact that necroptosis is closely related to tissue injury and inflammation (15), we explored whether necroptosis occurs during LPS-induced hepatic damage. TEM analysis of the ultrastructure of hepatocytes damaged by LPS has revealed mitochondrial swelling, endoplasmic reticulum expansion, nuclear deformation, nuclear membrane rupture, and chromatin overflow, all of which are consistent with the characteristics of necrosis. A time-dependent increase in

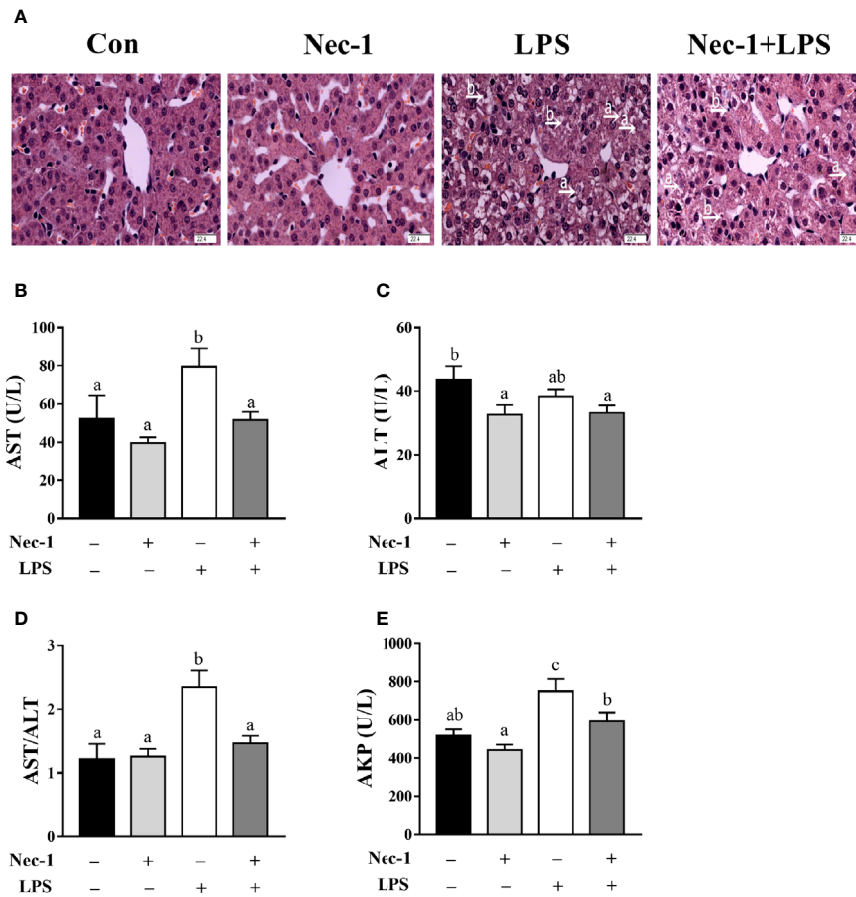


FIGURE 5 | Necrostatin-1 (Nec-1) prevents hepatic morphological damage and dysfunction in LPS-challenged piglets. Piglets were pretreated with Nec-1 at 1.0 mg/kg body weight or an equal volume of 2% DMSO 30 min before LPS or saline administration. Pigs were sacrificed at 4 h after LPS or saline injection. **(A)** Representative haematoxylin/eosin-stained liver sections. LPS induced hepatic histopathological changes such as hepatocyte caryolysis (a) and karyopycnosis (b), disordered hepatic cell cord arrangement, and hepatocyte vacuolation, but was obviously alleviated by Nec-1. Magnification: 400 ×, scale bars = 22.4 μm. **(B–E)** Serum AST, ALT and AKP activities and the AST/ALT ratio. Values are means ± SEM, n = 7. ^{abc} Means without a common letter differ significantly (p < 0.05).

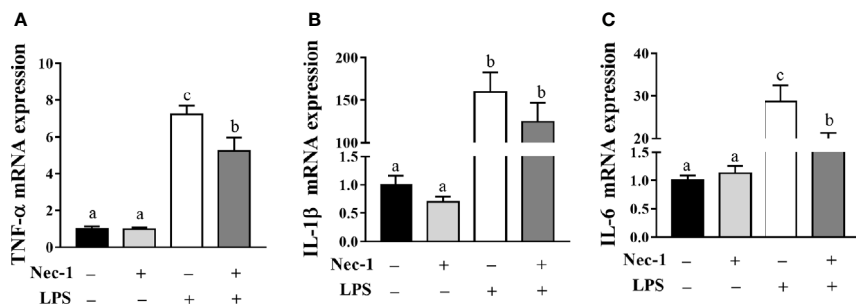


FIGURE 6 | Necrostatin-1 (Nec-1) reduces hepatic inflammation in LPS-challenged piglets. Piglets were pretreated with Nec-1 at 1.0 mg/kg body weight or an equal volume of 2% DMSO 30 min before LPS or saline administration. Pigs were sacrificed at 4 h after LPS or saline injection. **(A–C)** TNF-α, IL-1β and IL-6 mRNA expression in the liver. Values are means ± SEM, n = 7. ^{abc} Means without a common letter differ significantly (p < 0.05).

mRNA or protein expression levels of several critical components of necroptosis including RIP1, RIP3, MLKL, PGAM5, DRP1, and HMGB1 suggests the occurrence of necroptosis in the liver of LPS-challenged piglets. In agreement with our results, Shao et al. (28) showed that RIP1 protein was increased in a time-dependent manner in the brain cortex of LPS-challenged rats. In addition, Wang et al. (16) reported that LPS increased protein expression of RIP3, phosphorylated RIP3, and MLKL in the mouse lung 24 h post injection. Our results suggest that necroptosis may be induced quickly after LPS challenge and contribute to hepatic injury during sepsis.

To confirm the involvement of necroptosis in LPS-induced hepatic injury, Nec-1, a specific inhibitor of the RIP1 kinase activity and RIP1/RIP3 association (11, 23, 29), was used to inhibit necroptosis. Alleviation of ultrastructural hepatic necrotic changes by Nec-1 suggests that necroptosis is involved in LPS-induced liver injury. In addition, Nec-1 is capable of reducing the expression of RIP1 and MLKL as well as PGAM5, DRP1, and HMGB1 at mRNA or protein levels in the liver of LPS-treated pigs. Consistent with the involvement of necroptosis in liver damage, Nec-1 has been found to attenuate intestinal ischemia/reperfusion-induced liver injury (30). Inhibition of RIP1 by RIPA-56 alleviates experimental non-alcoholic fatty liver disease in mice (17). In addition, Knocking out the *Rip3* gene prevents ethanol-induced liver injury in mice (31). Our results demonstrate that necroptosis is involved in hepatic damage during sepsis.

Furthermore, we found that Nec-1 pretreatment decreased the mRNA abundance of hepatic TNF- α and IL-6, suggesting that necroptosis contributes to hepatic inflammation. Similarly, Takemoto et al. (32) reported that Nec-1 ameliorated hepatic IL-1 β , IL-6, IL-10, chemokine (C-X-C motif) ligand 1, and basic fibroblast growth factor expression in acetaminophen-induced acute liver failure in mice. Ni et al. (26) showed that targeting necroptosis by knocking out MLKL decreased hepatic neutrophil infiltration and inflammation in ischemia-reperfusion injury of murine steatotic livers. Our study demonstrates that necroptosis exacerbates inflammation in the liver of LPS-challenge piglets.

In our study, regrettably, the preformed experiments and obtained results were not in-depth enough, which might weaken their contributions in clinical medicine. Firstly, Nec-1 was used before the sepsis was induced (LPS challenge). It is unlikely that pretreatment with Nec-1 could be applied in clinical practice, which may limit the clinical use of Nec-1. Further research is needed to determine practical and effective clinical use regimens of Nec-1 after the sepsis. Secondly, only a single dose of Nec-1 was used in this study. In future studies, multiple

doses of Nec-1 should be evaluated to determine the optimal dose and therapeutic window of Nec-1 for maximal hepatic protection during sepsis.

In summary, we demonstrate that LPS activates necroptosis in the liver, resulting in the damage of hepatic structure and function. Targeting necroptosis with Nec-1 alleviates LPS-induced hepatic injury. Therefore, necroptosis occurs and contributes to hepatic damage during sepsis.

DATA AVAILABILITY STATEMENT

The raw data supporting the conclusions of this article will be made available by the authors, without undue reservation.

ETHICS STATEMENT

The animal study was reviewed and approved by the Animal Care and Use Committee of Wuhan Polytechnic University.

AUTHOR CONTRIBUTIONS

YL, C-AH, and GZ designed research. QX, JG, XL, YW, KX, XW, and HZ conducted research. YL, XL, and YW analyzed data. YL, DW, and QX wrote the paper. DW, C-AH, and GZ revised the manuscript. YL had primary responsibility for final content. All authors contributed to the article and approved the submitted version.

FUNDING

This research was financially supported by the Project of National Natural Science Foundation of China (No. 31772615), the Project of Innovative Research Groups of the Natural Science Foundation of Hubei Province (No. 2019CFA015), and Wuhan Science and Technology Bureau (No. 2018020401011304).

SUPPLEMENTARY MATERIAL

The Supplementary Material for this article can be found online at: <https://www.frontiersin.org/articles/10.3389/fimmu.2021.633830/full#supplementary-material>

REFERENCES

1. Angus DC, van der Poll T. Severe sepsis and septic shock. *N Engl J Med* (2013) 369:840–51. doi: 10.1056/NEJMra1208623
2. Cecconi M, Evans L, Levy M, Rhodes A. Sepsis and septic shock. *Lancet* (2018) 392:75–87. doi: 10.1016/S0140-6736(18)30696-2
3. Martin GS, Mannino DM, Eaton S, Moss M. The epidemiology of sepsis in the United States from 1979 through 2000. *N Engl J Med* (2003) 348:1546–54. doi: 10.1056/NEJMoa022139

4. Woźnica EA, Ingot M, Woźnica RK, Łysenko L. Liver dysfunction in sepsis. *Adv Clin Exp Med* (2018) 27:547–51. doi: 10.17219/acem/68363
5. Chen YL, Xu G, Liang X, Wei J, Luo J, Chen GN, et al. Inhibition of hepatic cells pyroptosis attenuates CLP-induced acute liver injury. *Am J Transl Res* (2016) 8:5685–95.
6. Luedde T, Kaplowitz N, Schwabe RF. Cell death and cell death responses in liver disease: mechanisms and clinical relevance. *Gastroenterology* (2014) 147:765–83. doi: 10.1053/j.gastro.2014.07.018

7. Mazzolini G, Sowa JP, Canbay A. Cell death mechanisms in human chronic liver diseases: a far cry from clinical applicability. *Clin Sci* (2016) 130:2121–38. doi: 10.1042/CS20160035
8. Schwabe RF, Luedde T. Apoptosis and necroptosis in the liver: a matter of life and death. *Nat Rev Gastro Hepat* (2018) 15:738–52. doi: 10.1038/s41575-018-0065-y
9. Saeed WK, Jun DW, Jang K, Koh DH. Necroptosis signaling in liver diseases: An update. *Pharmacol Res* (2019) 148:104439. doi: 10.1016/j.phrs.2019.104439
10. Sai K, Parsons C, House JS, Kathariou S, Ninomiya-Tsuji J. Necroptosis mediators RIPK3 and MLKL suppress intracellular *Listeria* replication independently of host cell killing. *J Cell Biol* (2019) 218:1994–2005. doi: 10.1083/jcb.201810014
11. Cho YS, Challa S, Moquin D, Genga R, Ray TD, Guildford M, et al. Phosphorylation-driven assembly of the RIP1-RIP3 complex regulates programmed necrosis and virus-induced inflammation. *Cell* (2009) 137:1112–23. doi: 10.1016/j.cell.2009.05.037
12. Moriwaki K, Farias Luz N, Balaji S, De Rosa MJ, O'Donnell CL, Gough PJ, et al. The mitochondrial phosphatase PGAM5 is dispensable for necroptosis but promotes inflammasome activation in macrophages. *J Immunol* (2016) 196:407–15. doi: 10.4049/jimmunol.1501662
13. Dong XH, Liu H, Zhang MZ, Zhao PX, Liu S, Hao Y, et al. Postconditioning with inhaled hydrogen attenuates skin ischemia/reperfusion injury through the RIP-MLKL-PGAM5/Drp1 necrotic pathway. *Am J Transl Res* (2019) 11:499–508.
14. Wang Z, Jiang H, Chen S, Du F, Wang X. The mitochondrial phosphatase PGAM5 functions at the convergence point of multiple necrotic death pathways. *Cell* (2012) 148:228–43. doi: 10.1016/j.cell.2011.11.030
15. Kearney CJ, Martin SJ. An inflammatory perspective on necroptosis. *Mol Cell* (2017) 65:965–73. doi: 10.1016/j.molcel.2017.02.024
16. Wang L, Wang T, Li H, Liu Q, Zhang Z, Xie W, et al. Receptor interacting protein 3-mediated necroptosis promotes lipopolysaccharide-induced inflammation and acute respiratory distress syndrome in mice. *PLoS One* (2016) 11:e0155723. doi: 10.1371/journal.pone.0155723
17. Majdi A, Aoudjehane L, Ratziu V, Islam T, Afonso MB, Conti F, et al. Inhibition of receptor-interacting protein kinase 1 improves experimental non-alcoholic fatty liver disease. *J Hepatol* (2020) 72:627–35. doi: 10.1016/j.jhep.2019.11.008
18. Yang F, Shang L, Wang S, Liu Y, Ren H, Zhu W, et al. TNF α -mediated necroptosis aggravates ischemia-reperfusion injury in the fatty liver by regulating the inflammatory response. *Oxid Med Cell Longev* (2019) 2019:2301903. doi: 10.1155/2019/2301903
19. Bassols A, Costa C, Eckersall PD, Osada J, Sabrià J, Tibau J, et al. The pig as an animal model for human pathologies: A proteomics perspective. *Proteom Clin Appl* (2014) 8:715–31. doi: 10.1002/prca.201300099
20. Roura E, Koopmans SJ, Lallès JP, Huerou-Luron IL, Jager ND, Schuurman T, et al. Critical review evaluating the pig as a model for human nutritional physiology. *Nutr Res Rev* (2016) 29:60–90. doi: 10.1017/S0954422416000020
21. Lee Y, Jeong GS, Kim KM, Lee W, Bae JS. Cudraticusxanthone A attenuates sepsis-induced liver injury via SIRT1 signaling. *J Cell Physiol* (2018) 233:5441–6. doi: 10.1002/jcp.26390
22. Wang LM, Tu ZX, Wang HB, Yang SH, Wang XY, Zhu HL, et al. Flaxseed oil improves liver injury and inhibits necroptotic and inflammatory signaling pathways following lipopolysaccharide challenge in a piglet model. *J Funct Foods* (2018) 46:482–9.
23. Degtrev A, Hitomi J, Germscheid M, Ch'en IL, Korkina O, Teng X, et al. Identification of RIP1 kinase as a specific cellular target of necrostatins. *Nat Chem Biol* (2008) 4:313–21. doi: 10.1038/nchembio.83
24. Wu H, Liu Y, Pi D, Leng W, Zhu H, Hou Y, et al. Asparagine attenuates hepatic injury caused by lipopolysaccharide in weaned piglets associated with modulation of TLR4 and NOD signaling and their negative regulators. *Br J Nutr* (2015) 114:189–201. doi: 10.1017/S0007114515001476
25. Livak KJ, Schmittgen TD. Analysis of relative gene expression data using real-time quantitative PCR and 2^{- $\Delta\Delta C_t$} method. *Methods*. (2001) 25:402–8.
26. Ni HM, Chao X, Kaseff J, Deng F, Wang S, Shi YH, et al. Receptor-interacting serine/threonine-protein kinase 3 (RIPK3)-mixed lineage kinase domain-like protein (MLKL)-mediated necroptosis contributes to ischemia-reperfusion injury of steatotic livers. *Am J Pathol* (2019) 189:1363–74. doi: 10.1016/j.ajpath.2019.03.010
27. Lang CH, Silvis C, Deshpande N, Nystrom G, Frost RA. Endotoxin stimulates in vivo expression of inflammatory cytokines tumor necrosis factor alpha, interleukin-1beta, -6, and high-mobility-group protein-1 in skeletal muscle. *Shock*. (2003) 19:538–46. doi: 10.1097/01.shk.0000055237.25446.80
28. Shao L, Liu X, Zhu S, Liu C, Gao Y, Xu X. The role of Smurf1 in neuronal necroptosis after lipopolysaccharide-induced neuroinflammation. *Cell Mol Neurobiol* (2018) 38:809–16. doi: 10.1007/s10571-017-0553-6
29. Deng XX, Li SS, Sun FY. Necrostatin-1 prevents necroptosis in brains after ischemic stroke via inhibition of RIPK1-mediated RIPK3/MLKL signaling. *Aging Dis* (2019) 10:807–17. doi: 10.14336/AD.2018.0728
30. Wen S, Li X, Ling Y, Chen S, Deng Q, Yang L, et al. HMGB1-associated necroptosis and Kupffer cells M1 polarization underlies remote liver injury induced by intestinal ischemia/reperfusion in rats. *FASEB J* (2020) 34:4384–402. doi: 10.1096/fj.201900817R
31. Roychowdhury S, McMullen MR, Pisano SG, Liu X, Nagy LE. Absence of receptor interacting protein kinase 3 prevents ethanol-induced liver injury. *Hepatology* (2013) 57:1773–83. doi: 10.1002/hep.26200
32. Takemoto K, Hatano E, Iwaisako K, Takeiri M, Noma N, Ohmae S, et al. Necrostatin-1 protects against reactive oxygen species (ROS)-induced hepatotoxicity in acetaminophen-induced acute liver failure. *FEBS Open Bio* (2014) 4:777–87. doi: 10.1016/j.fob

Conflict of Interest: The authors declare that the research was conducted in the absence of any commercial or financial relationships that could be construed as a potential conflict of interest.

Copyright © 2021 Xu, Guo, Li, Wang, Wang, Xiao, Zhu, Wang, Hu, Zhang and Liu. This is an open-access article distributed under the terms of the Creative Commons Attribution License (CC BY). The use, distribution or reproduction in other forums is permitted, provided the original author(s) and the copyright owner(s) are credited and that the original publication in this journal is cited, in accordance with accepted academic practice. No use, distribution or reproduction is permitted which does not comply with these terms.